

# Potential energy surfaces of substituted anilines: Conformational energies, deuteration effects, internal rotation, and torsional motion

R. Disselkamp, H. S. Im, and E. R. Bernstein

Citation: *The Journal of Chemical Physics* **97**, 7889 (1992); doi: 10.1063/1.463464

View online: <http://dx.doi.org/10.1063/1.463464>

View Table of Contents: <http://aip.scitation.org/toc/jcp/97/11>

Published by the [American Institute of Physics](#)

---

---

**COMPLETELY  
REDESIGNED!**



**PHYSICS  
TODAY**

*Physics Today* Buyer's Guide  
Search with a purpose.

# Potential energy surfaces of substituted anilines: Conformational energies, deuteration effects, internal rotation, and torsional motion

R. Disselkamp, H. S. Im,<sup>a)</sup> and E. R. Bernstein  
Colorado State University, Chemistry Department, Fort Collins, Colorado 80523

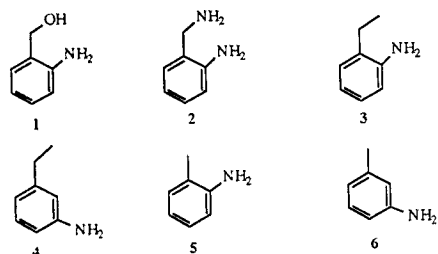
(Received 13 April 1992; accepted 17 August 1992)

Mass resolved excitation spectra (MRES) are presented for a series of substituted anilines including 2- and 3-methylaniline, 2- and 3-ethylaniline, 2-aminobenzyl amine, and 2-aminobenzyl alcohol. The observed spectra show the following phenomena: nearly free internal rotation of the methyl substituent in the  $S_1$  state; long vibrational progressions attributed to C-C, C-N, and C-O side chain torsional motion; an inequivalence of the two amino hydrogens for both ring and side chain amino groups as determined from the spectra of deuterated species; and the existence of two conformers for 2-aminobenzyl alcohol. Semiempirical and *ab initio* calculations are performed on these systems to aid in the analysis of the potential energy surfaces and in the interpretation of the experimental results.

## I. INTRODUCTION

If the potential energy surface of a molecule is known, molecular structure for a given electronic state can be calculated, and chemical reactivity estimated. Determination of the multidimensional potential energy surface for a molecule is typically a very difficult process, often initiated with only limited spectroscopic data. These data are usually restricted to the region of the potential energy minimum due to Franck-Condon constraints on spectroscopic transitions. In order to expand our information on potential energy surfaces fruitfully, calculations are an essential component of the overall approach. In principle, the experimentally accessed region of the potential can be examined to test various calculational algorithms and the acceptable algorithms can then be extended to generate the form of the surface in regions not readily accessible to experimental probing.

In this work we access spectroscopically the excited state ( $S_1$ ) potential surface of various substituted anilines 1-6 near the ground state ( $S_0$ ) equilibrium configuration with particular emphasis placed on that portion of the potential surface giving rise to low energy vibrational/torsional motion. Since in each case the data are collected by optical spectroscopy ( $S_1 \leftarrow S_0$ ) which is mass detected [mass resolved excitation spectroscopy (MRES)], the resulting spectra contain information on structural differences between the ground and first excited singlet states as well as excited state low energy modes of the various isotopically substituted molecules.



<sup>a)</sup>Korea Standard Research Institute, P. O. Box 3, Taeduck Science Toeun, Taejeon, Republic of Korea.

The nature of the experimental approach taken here has already been presented for the 2-aminobenzyl alcohol system.<sup>1</sup> In that case, 2-amino- $d_0$ ,  $d_1$ ,  $d_2$ -benzyl alcohol- $d_0$ ,  $d_1$  molecules were studied by MRES. We conclude from those spectra that the two amino hydrogen atoms are not equivalent, the low energy modes involved torsional motion of the  $-\text{CH}_2\text{OH}$  group, and the ground and excited states have different geometries in the region of the substituents. To explore the nature of the isotopic energy differences observed for 2-aminobenzyl alcohol further, we now extend the experimental investigation to include other molecules of similar typology (1-6) and augment the experimental program with *ab initio* and semiempirical quantum mechanical calculations, and molecular force field calculations. Our results suggest that interactions between the ring amino group and the side chain  $\text{CH}_2\text{OH}$ ,  $-\text{CH}_2\text{NH}_2$ ,  $-\text{CH}_3$ , and  $-\text{CH}_2\text{CH}_3$  substituents of the benzene ring are largely steric in nature. In addition, one-dimensional potential energy surfaces for various internal subgroup motion (e.g., methyl rotation and side chain torsion motion) are determined.

## II. EXPERIMENTAL PROCEDURES

All data reported in this study are one-color mass resolved excitation spectra (MRES) obtained using a one plus one photon resonance enhanced ( $S_1 \leftarrow S_0$ ) ionization. A complete description of the experimental procedure can be found in a previous publication from this laboratory.<sup>2</sup> The frequency doubled output of a Nd:YAG pumped dye laser was focused into the ion extraction region of a time-of-flight mass spectrometer. Kiton red dye was used for the methyl and ethyl substituted anilines and rhodamine 640 dye was used for the 2-aminobenzyl alcohol/amine species. The laser output was made to intersect the cold beam of molecules generated by skimming the output from an R. M. Jordan pulsed nozzle operating at 10 Hz. Helium was used as an expansion gas with a total backing pressure of roughly 50 psi. All samples were placed in the nozzle and not further heated. Nozzle temperature under operating conditions was 30 °C. As laser energy was scanned the organic molecules underwent two photon excitations

( $I \leftarrow S_1 \leftarrow S_0$ ) to generate ions. The ion current measured reflected the  $S_1 \leftarrow S_0$  "absorption" spectrum. Up to four separate spectra of various isotopes of a given molecule were recorded simultaneously through different box car integrator channels. The "negative peaks" in some of the recorded spectra (see Figs. 4, 6, 8, and 9) are due to intense signals appearing in lower mass channels ringing into the observed mass channel. Nondeuterated samples were purchased from Aldrich Chemical Co. Hydroxy and amino deuteration was accomplished by standard exchange with  $D_2O$  followed by ether extraction. Methyl deuterated compounds were provided by Seeman and Secor.<sup>3</sup>

### III. THEORETICAL AND CALCULATIONAL PROCEDURES

The compounds studied here are spectroscopically quite complex, therefore we restrict our attention to low energy torsional motion, methyl rotor motion, and isotopic spectral shifts as a function of isotope substitution. To aid in the analysis of our experimental results, we perform various calculations: semiempirical molecular orbital calculations of ground state energies and structures; *ab initio* Hartree-Fock calculations of ground state energies and structures; molecular force field calculations of energies, structures, and vibrations; and the determination of one-dimensional methyl rotor potential energy surfaces.

#### A. Molecular orbital calculations

Both semiempirical and *ab initio* calculations were performed to determine ground state conformational energies and structures of the various molecules of interest. These calculations were performed on an IBM RISC/6000 computer system equipped with 24 MB of memory. For the methylanilines, only a single equilibrium methyl group conformation is predicted. For the remaining systems, multiple equilibrium conformations are calculated, each of which we will examine in detail in the ensuing discussion as possible realizable structural conformers.

Semiempirical calculations were carried out using the MOPAC 6 series of programs.<sup>4</sup> Conformational energies were obtained using the PM3 Hamiltonian for a specific structure using a two step geometry optimization technique. First, a molecule's structure was partially optimized by performing a non-linear least squares (NLLSQ) energy gradient minimization. Second, a subsequent structure optimization was carried out through the use of an eigenvalue following (EF) routine. For 3-ethylaniline, the ethyl group torsional potential was mapped out relative to the aromatic ring plane by optimizing all degrees of freedom as described above except for the torsional angle of interest.

*Ab initio* calculations were carried out for these molecules using the GAUSSIAN 88 molecular orbital package.<sup>5</sup> Ground state restricted Hartree-Fock geometry optimizations were performed for the methylanilines and for only a select few of the lowest energy conformational structures, as determined from MOPAC 6, of the remaining compounds. MOPAC optimized geometries were used as input for the *ab initio* calculations which used a 6-31G\* split valence basis

set. Energy gradients were reduced to less than  $10^{-5}$  Hartree/Bohr in the calculations.

Molecular force field calculations were performed to determine vibrational frequencies using the WERK molecular mechanics package developed by A. K. Rappé *et al.*<sup>6</sup> Partial charges evaluated by the *QeQ2* algorithm were included in the calculations discussed here. Conformational energies were optimized by reducing energy gradients to less than  $10^{-10}$  (kcal/mol)/Å which resulted in residual vibrations less than  $10^{-3}$   $\text{cm}^{-1}$ .

#### B. Internal methyl rotation

In the next section, spectroscopic features of 2-methylaniline will be identified which strongly suggest that the methyl group is undergoing nearly free rotation. Because of this, we present the pertinent background needed to model such spectra. Internal rotation is a subject which has been extensively studied,<sup>7-12</sup> therefore only a brief overview of the theory needed to describe such phenomena will be presented here.

The one-dimensional Hamiltonian describing restricted internal rotation within a molecule can be written as

$$H = -B(d^2/d\phi^2) + V(\phi) \quad (1)$$

in which  $\phi$  is the torsional angle,  $B$  is the effective rotational constant expressed in wave numbers, and  $V(\phi)$  is the potential energy function describing the restricted motion. For a free rotor,  $V(\phi) = 0$  and the energy levels simply become  $E = m^2B$ , with  $m = 0, 1, 2, 3, \dots$ . In general,  $V(\phi)$  can be expressed in terms of a cosine expansion

$$V(\phi) = \sum_n [V_n/2] (1 - \cos(n\phi)) \quad (2)$$

For the methyl top internal rotation of concern here,  $B = 5.2 \text{ cm}^{-1}$ , and the potential energy function becomes

$$V(\phi) = V_3/2(1 - \cos 3\phi) + V_6/2(1 - \cos 6\phi) + \dots \quad (3)$$

The eigenfunctions and eigenvalues of the Hamiltonian defined by Eqs. (1) and (2) can be found by choosing an appropriate trial wave function, constructing the secular determinant for  $H$ , and diagonalizing. A basis set often chosen for matrix element evaluation is

$$\Psi_{\text{total}} = \Psi_{\text{even}} + \Psi_{\text{odd}}$$

in which

$$\Psi_{0 \text{ even}} = 1/(2\pi)^{1/2},$$

$$\Psi_{n \text{ even}} = (1/\pi)^{1/2} \cos(n\phi) \quad n = 1, 2, 3, \dots, N,$$

$$\Psi_{n \text{ odd}} = (1/\pi)^{1/2} \sin(n\phi) \quad n = 1, 2, 3, \dots, N. \quad (4)$$

The appropriate matrix elements involving these basis functions can be found in Table 3 of Ref. 9. The basis set size,  $N$ , must be sufficiently large to assure convergence of the calculated energies and wave functions. For the modeling we present here, the resulting secular determinant is block diagonal due to the symmetry of the potential function and basis set. The even block involves cosine basis set functions while the odd block involves only sine basis set functions. The calculated energies in increasing order correspond to  $m=0,1,2,3,\dots$  for the even block and  $m=1,2,3,\dots$  for the odd block. In practice, the observed rotor transitions are fit to a set of potential energy constants  $V_3$ ,  $V_6$ , etc. through an iterative procedure.

The observed transitions can be accounted for by using wave function symmetries ( $\Gamma_{el}$ ,  $\Gamma_{nuc}$ ,  $\Gamma_{rot}$ , etc.) to determine the allowed and forbidden transitions between the calculated states. Detailed discussions describing this procedure are given elsewhere.<sup>16,17</sup> Briefly, one first identifies the permutation-inversion molecular symmetry group appropriate for the potential function modeling the internal rotation, then transforms the rotor wave functions under the operations of this group to obtain the desired irreducible representations pertaining to each torsional quantum number  $m$ . For a potential function constructed from  $V_3$  and  $V_6$  terms the appropriate permutation-inversion molecular symmetry group is either  $G_3^1$  or  $G_6^2$ , whereas for a purely sixfold potential the appropriate molecular symmetry group is  $G_{12}$ .<sup>17</sup> The transition is considered to be electronic in nature.

#### IV. RESULTS AND DISCUSSION

A major theme of the research reported here deals with the structure of, and interaction between, the aromatic amino group and ortho or meta substituents. Molecular structure becomes especially interesting if two identifiable groups (e.g.,  $\text{NH}_2$  and  $-\text{CH}_2\text{R}$ ) can interact with one another to varying degrees. The nonrigidity, structure, and perhaps solvation and chemical properties of molecules may be significantly altered by such internal interactions. In presenting the experimental and calculational results for the 2-aminobenzyl alcohol and amine, and the 2,3-methyl and ethyl substituted anilines, we will begin with the already published experimental data for 2-aminobenzyl alcohol and use the ensuing studies in part to elaborate and to explore the interactions and potential energy surfaces of this system.

##### A. 2-aminobenzyl alcohol

Figures 1 and 2 present the MRES of 2-aminobenzyl alcohol- $d_0$ ,  $d_1$ ,  $d_2$ ,  $d_3$  isotopomers for the readily exchangeable  $-\text{OH}$  and  $-\text{NH}_2$  hydrogens.<sup>1</sup> A clear 1/3/3/1 deuteration pattern exists among the spectroscopic features for these randomly deuterated species. One can immediately extract the following information from these spectra: Since the  $d_1$  and  $d_2$  spectra of Fig. 1 show three features for each single feature of the  $d_0$  and  $d_3$  spectra, the amino hydrogens and one hydroxy hydrogen must be inequivalent; the observed spectra are probably due to two conformers of

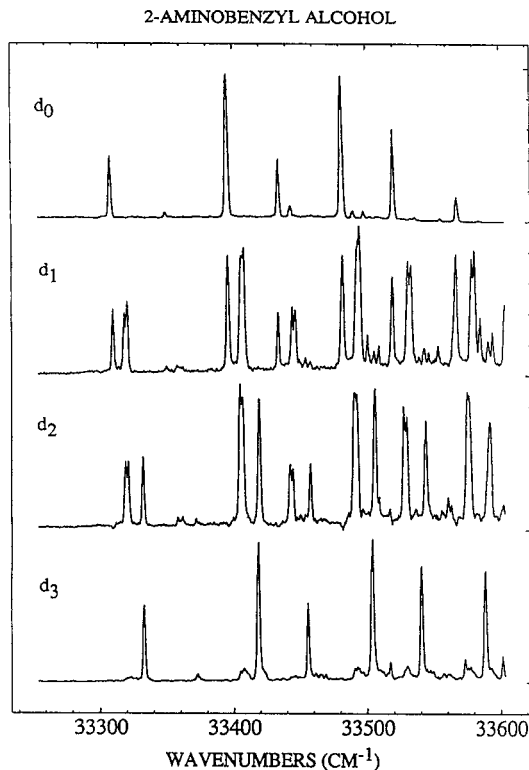


FIG. 1. Mass resolved excitation spectra (MRES) of the origin region of amino and hydroxy isotopomers of 2-aminobenzyl alcohol. The unresolved doublet origin features for  $d_1$  are assigned to  $-\text{NHD}$ ,  $-\text{NDH}$  deuteration and the remaining lone feature corresponds to isotope substitution of the hydroxy group.

2-aminobenzyl alcohol, one with an origin transition at  $33\,311\text{ cm}^{-1}$  ( $-d_0$ ) and the other at  $33\,351\text{ cm}^{-1}$  ( $-d_0$ ) (a single conformer interpretation of these spectra would require that the progression spacing oscillate between 45

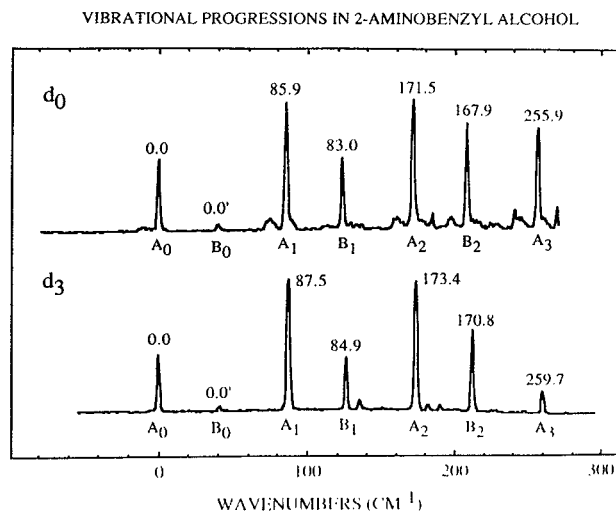
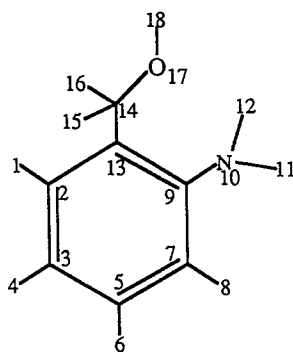


FIG. 2. Expansion of the  $d_0$  and  $d_3$  origin spectra of Fig. 1. The effect of amino and hydroxy deuteration ( $d_0$  and  $d_3$ ) on the vibrational progressions of 2-aminobenzyl alcohol can be seen to blue shift the observed vibrations. Progressions corresponding to two conformations ( $A_0$  and  $B_0$ ) are believed to exist.

TABLE I. MOPAC 6 and *ab initio*<sup>a</sup> conformational energies of 2-aminobenzyl alcohol.

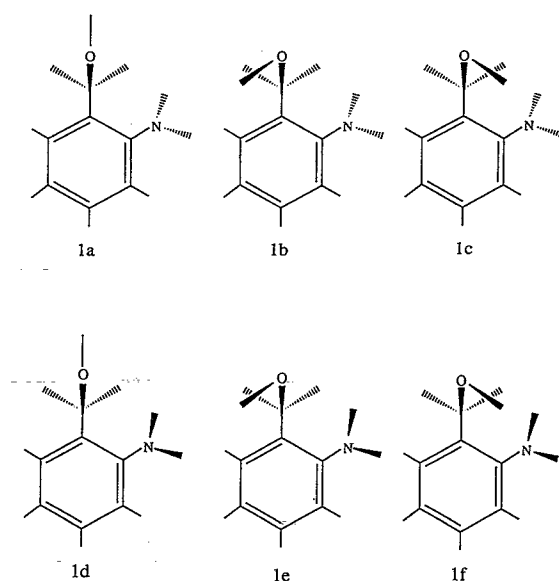
Molecular property	Structure 1 <sup>b</sup>					
	a	b	c	d	e	f
<b>MOPAC:</b>						
Absolute energy (a.u.)	-52.330 32	-52.335 44	-52.335 77	-52.331 58	-52.335 76	-52.333 69
Relative energy (cm <sup>-1</sup> )	1194.4	71.8	0.0	920.0	0.9	456.9
<b>Ab initio:</b>						
Absolute energy (a.u.)	...	-399.614 880	-399.613 870	...	-399.617 866	...
Relative energy (cm <sup>-1</sup> )	...	655.4	877.1	...	0.0	...

<sup>a</sup>6-31G\* basis set.<sup>b</sup>See Fig. 3.

and 35 cm<sup>-1</sup> and that the odd transitions of this mode are somehow forbidden); each origin  $A_0$  and  $B_0$  of the two conformers of Fig. 2 each has a low frequency progression built on it of 86 and 83 cm<sup>-1</sup>, respectively; the Franck-Condon factors for the excited state displacement in this (assumed) common mode are somewhat different for each conformer.

To proceed further with the analysis, calculations are essential. Both semiempirical and *ab initio* calculations are performed for 2-aminobenzyl alcohol and are presented in Table I. In all calculations, the oxygen atom retains an  $sp^3$  hybridization. Six possible conformers for this molecule are shown in Fig. 3. Two additional conformers with the -CH<sub>2</sub>OH moiety in the plane of the ring are not stable. Semiempirical MOPAC 6 calculations predict conformers **1c** and **1e** to be isoenergetic, with structure **1b** only slightly higher in energy. Conversely, *ab initio* calculations predict that conformer **1e** is lowest in energy. Since two conformers are observed experimentally, the *ab initio* calculations are inconsistent with this result. We suggest based on the semiempirical results that conformers **1e** and **1c** are observed, with **1b** a possible contender. The uncertainty in conformational structure arising from the calculational results makes this molecule an interesting candidate for future study using high resolution spectroscopic techniques. WERK force field calculations predict identical vibrational modes for these conformers. The lowest frequency vibrations for conformation **1c** are the C-O side chain torsional

## 2-Aminobenzyl Alcohol Conformations

FIG. 3. Geometric conformations of 2-aminobenzyl alcohol. Table I lists the semiempirical and *ab initio* calculated energies for these structures.

motion relative to the aromatic ring ( $\alpha_{17-14-13-9}$ ) occurring at  $103\text{ cm}^{-1}$  followed by the C–O side chain bend into the plane of the aromatic ring at  $155\text{ cm}^{-1}$  (bend occurs at carbon 13, see Table I). Vibrations calculated for conformers **1e** and **1b** agree to within  $5\text{ cm}^{-1}$  of those for **1c**. The observed, albeit excited state, progressions of  $86$  and  $83\text{ cm}^{-1}$  are in good agreement with these predictions. This motion clearly is not due to hydrogen motion alone, as can be seen from its vanishingly small isotope effect (see Figs. 1 and 2).

The MOPAC calculated structures for conformers **1e** and **1c** show that the two hydrogens attached to the amino group of the aromatic ring are not equivalent. The out-of-plane angles differ by  $3^\circ$  for these two conformers ( $\alpha_{12-10-9-7}$  and  $\alpha_{11-10-9-7}$ , see Table I). This fact is also clear from the spectrum of the isotopic 2-aminobenzyl- $d_1$ , - $d_2$  alcohols. The calculations for 2-aminobenzyl alcohol do not address the magnitude of this observed inequivalency which likely arises from the zero point energy difference between the –NHD and –NDH conformers in the two electronic states  $S_0$  and  $S_1$ . Nonetheless, one might speculate that hydrogen bonding interactions play a role in this energy difference. A hint that this might *not* be the case can be obtained from a comparison of the isotope effect observed for the two conformers identified for the 2-aminobenzyl alcohol- $d_0$ ,  $d_1$ ,  $d_2$  species. Figures 1 and 2 make clear that these shifts and splittings are nearly identical even though the computationally assigned structures are significantly different with regard to hydrogen bonding.

The question now arises as to the assignment of the 2-aminobenzyl alcohol- $d_1$  and - $d_2$  features for the  $0_0^0$  transition in Fig. 1: Is the single feature in these spectra due to the NHD or the OH/OD moiety? The overall blue shift upon OH and  $\text{NH}_2$  deuteration of 2-aminobenzyl alcohol is  $25\text{ cm}^{-1}$ . Data for deuteration in benzyl alcohol,<sup>1</sup> 2- and 3-methylaniline, 2- and 3-ethylaniline (see discussion below), and benzyl amine<sup>18</sup> shows that double deuteration at the position  $\alpha$  to the ring yields spectral blue shifts of ca.  $20\text{ cm}^{-1}$ , while deuteration at the position  $\beta$  to the ring yields little or no ( $<4\text{ cm}^{-1}$ ) blue shift. Hence, we suggest that the 2-aminobenzyl alcohol- $d_1$  and - $d_2$  origin features that are well resolved, single peaks, are due to the alcohol deuterated molecules in both instances. Consequently, the unresolved doublets in both cases arise from the amino deuterated species.

To explore the internal hydrogen bonding proposition further, we next investigate 2-aminobenzyl amine which should have smaller internal hydrogen bonding interactions followed by the 2-, 3-ethyl- and 2-, 3- methylanilines which should not have any internal hydrogen bonding interactions.

## B. 2-aminobenzyl amine

The spectra of the  $d_0$ – $d_4$  amino group isotopically substituted aminobenzyl amines (**2**) are presented in Figs. 4 and 5. The vibronic transitions of this species (i.e.,  $0_0^0$ ,  $X_0^n$ ,  $Y_0^n$ ,  $Z_0^n$ ) are all “split” into a 1/4/6/4/1 deuteration pattern for the randomly isotopically exchanged species. These spectra are of the same nature as those found for the

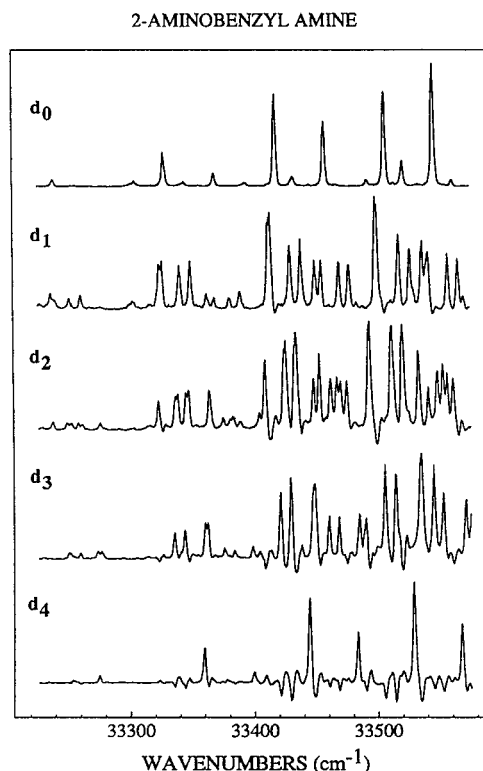


FIG. 4. MRES of the origin region of amino deuterated isotopomers of 2-aminobenzyl amine.

2-aminobenzyl alcohol system. Now, however, four positions are available for random isotopic substitution among four inequivalent sites, hence the expected 1/4/6/4/1 pattern emerges for the  $d_0$ – $d_4$  deuteration, respectively. The assignment of the various features comprising the  $0_0^0$  transitions for each isotopomer cannot be made uniquely; nonetheless, a hint as to the origin of these features can be taken from the 2-aminobenzyl alcohol results. In that instance, the largest isotopic shift came from ring amino deuteration. Assuming that this shift pattern also exists for 2-aminobenzyl amine, we can assign the higher energy doublet to the ring amino- $d_1$  and the lower energy less resolved doublet to the benzyl amine amino- $d_1$ . The  $d_3$  spectra have a like interpretation for the two doublets: the higher energy doublet is due to the benzyl amine amino- $d_1$  and the lower energy doublet is due to the ring amino- $d_1$ . The  $d_2$  isotopomer transitions are assigned as follows: The lowest energy singlet is due to the benzyl amine amino- $d_2$ , and the highest energy singlet is due to the ring amino- $d_2$ . The two central doublets are not obviously assigned by this scheme since each group has one deuterium atom. The subtlety of this isotope effect is illustrated by the latter  $d_2$  substitution on 2-aminobenzyl amine. Note that this assignment is not unique and other internally consistent schemes can be generated. The one presented here is based on the size of the isotope shifts found for molecules of similar typology.

Since the difference between the transition energies of the various isotopomers  $d_0$  through  $d_4$  for 2-aminobenzyl

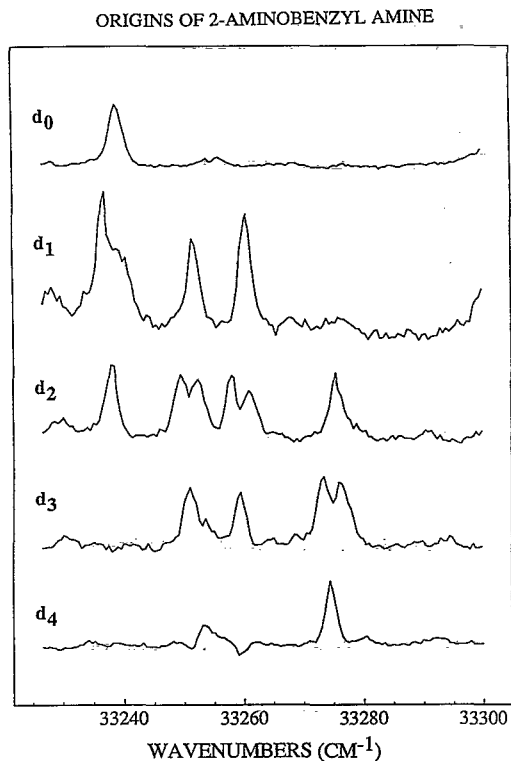


FIG. 5. Expansion of the  $S_0 \rightarrow S_1$  origin region of 2-aminobenzyl amine (see Fig. 4). Deuteration of the four inequivalent amino hydrogen sites leads to an expected 1:4:6:4:1 deuteration pattern.

amine is actually larger than that found for 2-aminobenzyl alcohol (ca. 35 vs 20  $\text{cm}^{-1}$ ), one can tentatively conclude that the inequivalence of the isotopomer transitions is not directly related to hydrogen bonding, as the hydrogen bond for  $-\text{OH} \cdots \text{NH}_2$  must surely be stronger than that for  $-\text{NH}_2 \cdots \text{NH}_2$ .

The vibronic spectrum of 2-aminobenzyl amine can also be analyzed to some extent in the region of the  $0_0^0$  transition. As indicated in Fig. 6, three progressions can be identified built on the 2-aminobenzyl amine- $d_0$  origin transition at 33 238  $\text{cm}^{-1}$ . The fundamentals of these progressions are located at 64.5  $\text{cm}^{-1}$  ( $B_1$ ), 88.5  $\text{cm}^{-1}$  ( $A_1$ ) and 104.6  $\text{cm}^{-1}$  ( $C_1$ ). Each progression has its own Franck-Condon factor and its own anharmonicity: The progression  $A_n$  has an intensity maximum at  $A_2$  to  $A_3$  and is harmonic; the progression  $B_n$  has an intensity maximum at  $B_2$  and the  $B_5$ - $B_4$  anharmonicity is only +4  $\text{cm}^{-1}$ ; the progression  $C_n$  has an intensity maximum at  $C_3$  or  $C_4$  and a  $C_3$ - $C_2$  anharmonicity of -4  $\text{cm}^{-1}$ . The regularity of these progressions and the small anharmonicities suggest that only one conformer is present for this system.

Calculations for 2-aminobenzyl amine are carried out using both semiempirical and *ab initio* algorithms, the results of which are given in Table II. Both sets of results agree that **2a** is the minimum energy structure (see Fig. 7) and that only one lowest energy conformer is present. Note that the lowest energy conformer for 2-aminobenzyl amine

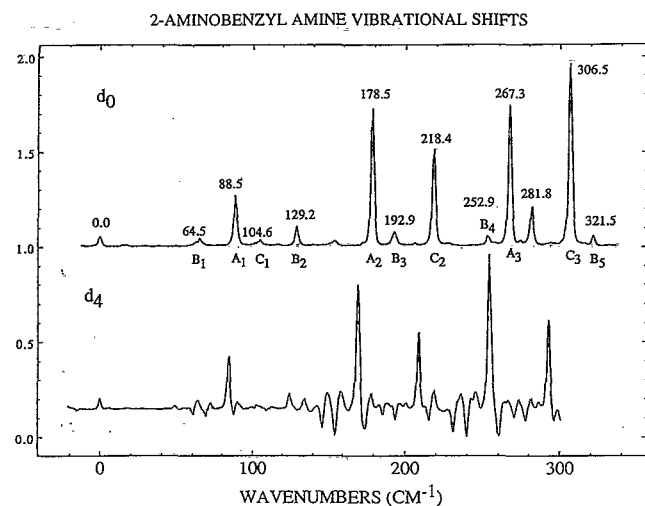


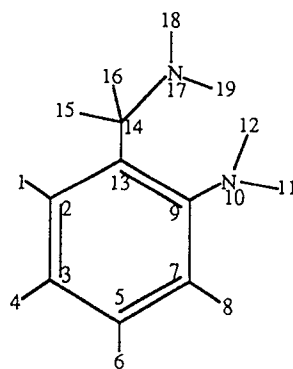
FIG. 6. The effect of complete amino deuteration on the vibrational progressions of 2-aminobenzyl amine (see Fig. 4). The top spectrum shows an assignment of three vibrational progressions belonging to one conformer.

is the one that has maximal hydrogen bonding between the two amine groups as well as strong bonding between the  $-\text{CH}_2\text{NH}_2$  group and the aromatic  $\pi$  system.

The WERK molecular mechanics program was used to calculate the vibrational frequencies of the lowest energy structure **2a** in Fig. 7. Partial charges were included in the calculation. The three lowest (ground state) vibrational frequencies correspond to a torsional motion of the benzyl amine group relative to the plane of the aromatic ring ( $\alpha_{17-14-13-9}$ ) at 109  $\text{cm}^{-1}$ , a bending of the benzyl amine group into the plane of the aromatic ring (bending at carbon 14, see Table II) at 148  $\text{cm}^{-1}$ , and a twisting of the ring amino group at 208  $\text{cm}^{-1}$ . The first two calculated vibrations correspond to essentially the same side chain motion as in the aminobenzyl alcohol system. The disagreement between the calculated and observed frequencies here, however, makes a unique assignment problematical. These inconsistencies arise from either a dramatic change in the potential surface upon electronic excitation, or subtleties of amino group-aromatic ring interactions not yet accounted for in the theory, or both. Note too, that the  $d_0/d_4$  isotope effects are not dramatic enough to aid in an assignment, probably due to mode mixing and similarity (see Fig. 6).

### C. 2-ethylaniline and 3-ethylaniline

Special interactions between the two substituent groups such as intramolecular hydrogen bonding and side chain -  $\pi$ -system interactions can be further reduced by replacing the  $-\text{CH}_2\text{NH}_2$  or  $-\text{CH}_2\text{OH}$  substituents by a saturated hydrocarbon. Moreover, by studying 2-,3-ethylaniline one can explore the nature, strength, and distance dependence of the interactions giving rise to the

TABLE II. MOPAC 6 and *ab initio*<sup>a</sup> conformational energies of 2-aminobenzyl amine.

Molecular property	Structure 2 <sup>b</sup>					
	a	b	c	d	e	f
<b>MOPAC:</b>						
Absolute energy (a.u.)	-48.071 40	-48.067 84	-48.067 37	-48.070 50	-48.066 13	-48.068 31
Relative energy (cm <sup>-1</sup> )	0.0	782.4	884.1	197.3	1156.4	677.9
<b>Ab initio:</b>						
Absolute energy (a.u.)	-379.785 839	...	...	-379.782 915	...	...
Relative energy (cm <sup>-1</sup> )	0.0	...	...	641.8	...	...

<sup>a</sup>6-31G\* basis set.<sup>b</sup>See Fig. 7.

## 2-ETHYLANILINES

## 2-Aminobenzyl Amine Conformations

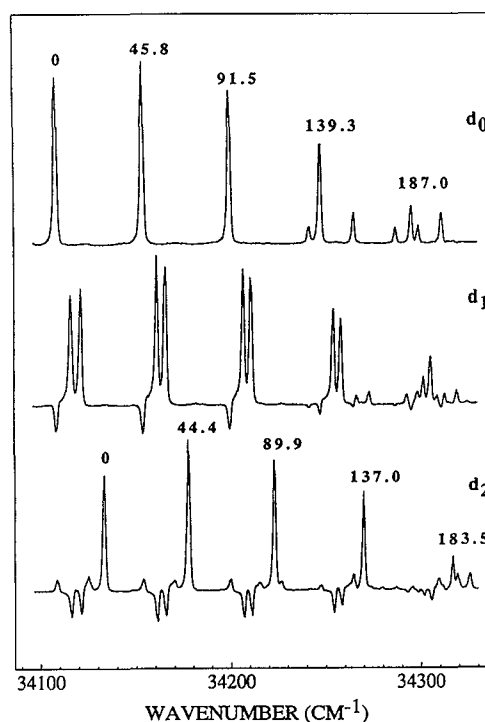
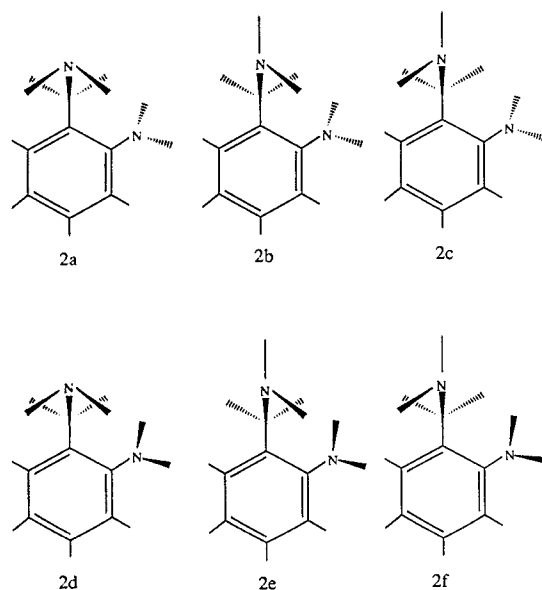
FIG. 7. Geometric conformations of 2-aminobenzyl amine. Table II lists semiempirical and *ab initio* calculated energies for these structures.

FIG. 8. MRES of the origin region of amino deuterated isotopomers of 2-ethylaniline.

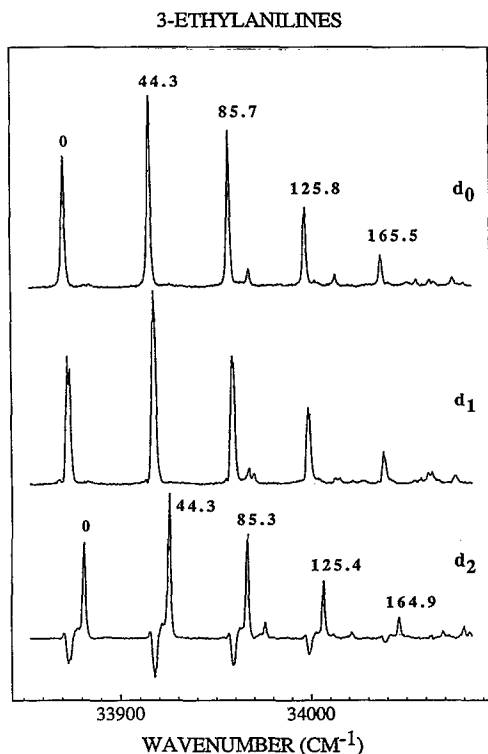


FIG. 9. MRES of the origin region of amino deuterated isotopomers of 3-ethylaniline.

—NHD/—NDH inequivalence. In these two “simplified” molecules, the two substituent groups can be either *syn* or *anti* to the amino group in their lowest energy conformations.

Spectra for 2- and 3-ethylaniline- $d_0$ ,  $d_1$ ,  $d_2$  are presented in Figs. 8 and 9. Note that the size of the —NHD/—NDH isotopomer energy difference for 2-ethylaniline- $d_1$  is roughly half that found for the benzyl amine and benzyl alcohol deuteration discussed above, and that the ring amino deuteration of these species is again likely to be the major contributor to the  $d_0/d_3$ ,  $d_0/d_4$ , and  $d_0/d_2$  isotope shifts, respectively. While a definite assignment of spectroscopic features cannot be made, the vibronic torsional progressions of ca.  $45\text{ cm}^{-1}$  for 2,3-ethylaniline- $d_0$ ,  $d_1$ ,  $d_2$  are seen to be independent of both substituent position (i.e., ortho vs meta) and deuteration. The harmonic nature of the vibrational progressions also implies only a single lowest energy conformation exists. The —NHD/—NDH spectroscopically observed inequivalence is much smaller for 3-ethylaniline as would be expected for simply a steric effect: Even in the *meta* position, the amino group can sense the presence of the ethyl substituent.

Figure 10 lists the conformations investigated for 2-ethylaniline. Table III presents the conformational energies using the two calculational algorithms. Although structures **3c** and **3d** are maxima on the side chain torsional potential energy surface, only the *ab initio* calculated structure **3c** converts to a local minimum. Due to similarities in the *ab initio* and MOPAC determined structures, only the *ab initio* results are listed in Table III. Both calculations pre-

## 2-Ethylaniline Conformations

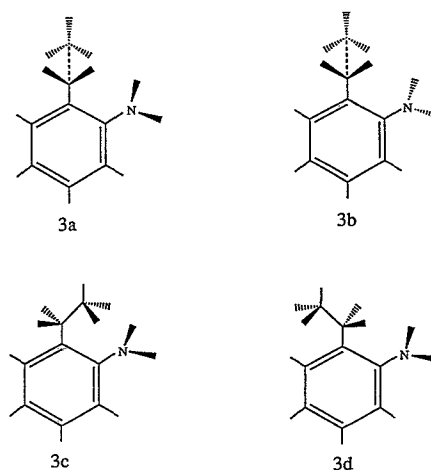


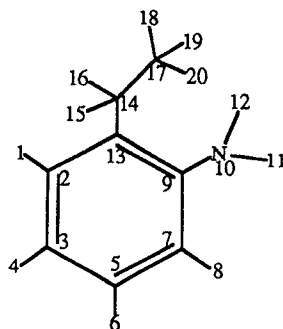
FIG. 10. Geometric conformations of 2-ethylaniline. Table III lists semi-empirical and *ab initio* calculated structures and energies for these structures.

dict the same results: the “perpendicular” *anti*-conformation **3a** is lowest in energy and the “perpendicular” *syn*-conformation **3b** is roughly  $100\text{ cm}^{-1}$  higher in energy. The inequivalence of the amino hydrogens can be seen in the angles  $\alpha_{12-10-9-13}$  and  $\alpha_{11-10-9-7}$ .

Essentially the same calculational picture emerges for 3-ethylaniline. Figure 11 lists structural conformations while Table IV presents the calculated energies and geometries. The *anti*-conformer **4a** is predicted to be slightly lower in energy. The *syn*- and *anti*-conformers are nearly degenerate in energy which is inconsistent with the experimental observation of one conformer. The ethyl group is calculated to be more perpendicular to the aromatic ring than 2-ethylaniline, and the —NH<sub>2</sub> bonds are nearly equivalent. The ethyl torsional barrier calculated from MOPAC is  $400\text{ cm}^{-1}$ .

WERK force field calculations of the vibrations of 2-, 3-ethylaniline indicate that the lowest frequency vibration for both species is the ethyl group torsion relative to the aromatic ring plane ( $\alpha_{17-14-13-9}$  for 2-ethylaniline and  $\alpha_{17-14-13-11}$  for 3-ethylaniline) of  $71$  and  $83\text{ cm}^{-1}$ , respectively. The next higher frequency vibrations again are identical for each species and correspond to the ethyl group torsion toward the plane of the aromatic ring of roughly  $150\text{ cm}^{-1}$ . Thus, the calculated lowest frequency vibrations for all side chain species C—O, C—N, and C—C discussed thus far are calculated to be identical in type of vibration and similar in frequency.

An interesting comparison to make is the relative stability, or total energy, of 2- vs 3-ethylaniline. Tables III and IV show that 3-ethylaniline is roughly  $500\text{ cm}^{-1}$  more stable than 2-ethylaniline. This small energy difference is consistent with a repulsive, or steric, interaction.

TABLE III. Conformational energies and structures of 2-ethylaniline.<sup>a</sup>

Molecular property	Structure 3 <sup>b</sup>			
	a	b	c	d
<i>Ab initio:</i>				
Absolute energy (a.u.)	-363.800 372	-363.800 072	...	-363.799 011
Relative energy (cm <sup>-1</sup> )	0.0	65.9	...	298.7
MOPAC 6:				
Absolute energy (a.u.)	-47.038 635	-47.037 946	-47.030 131	-47.036 013
Relative energy (cm <sup>-1</sup> )	0.0	151.2	1866.6	575.5
<i>Ab initio:</i>				
Internal Angles (degrees)				
$\alpha_{12-10-9-13}$	32.1	-35.6	...	36.1
$\alpha_{11-10-9-7}$	20.4	-16.9	...	16.4

<sup>a</sup>6-31G\* basis set.<sup>b</sup>See Fig. 10.

## D. 2-methylaniline and 3-methylaniline

These compounds are the simplest of the series; namely, no *syn*- or *anti*-conformers should exist. Figure 12 presents the spectra of the amino-deuterated 2-methylanilines. From these spectra we note the following two conclusions: the -NHD/-NDH inequivalency exists for this compound with almost the same spectral shifts observed for the other three systems; and the methyl group is bound in the ground state but relatively free in the first excited state. The latter conclusion arises from the weak features following the origin. The spectra are similar to those found for *meta*- and *para*-xylene,<sup>12</sup> toluene,<sup>12,13</sup> and *meta*- and *para*-fluorotoluene.<sup>14,15</sup> A further demonstration of relatively free methyl group internal rotation in  $S_1$  is given in Fig. 13 which presents the spectrum of 2-methyl- $d_0$ -,  $d_3$ -aniline about the  $0_0^0$  transition. The characteristic reduction in rotor transition energy relative to the origin by roughly a factor of two upon deuteration supports the assertion. (Recall for a free rotor the energy levels are equal to  $m^2B$  in which  $m$  is an integer quantum number

## 3-Ethylaniline Conformations

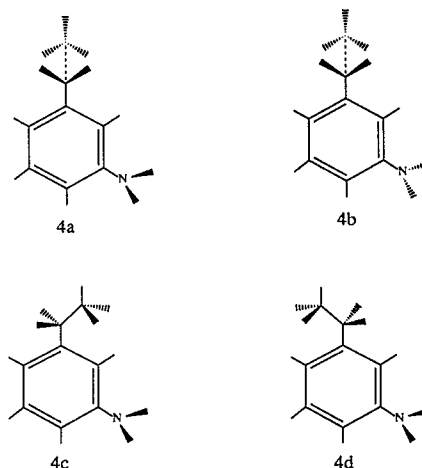
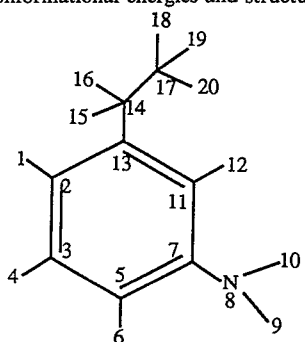
FIG. 11. Geometric conformations of 3-ethylaniline. Table IV lists semi-empirical and *ab initio* calculated structures and energies for these structures.

TABLE IV. Conformational energies and structures of 3-ethylaniline.<sup>a</sup>

Molecular property	Structure 4 <sup>b</sup>			
	a	b	c	d
<i>Ab initio:</i>				
Absolute energy (a.u.)	-363.802 830	-363.802 802	-363.800 464	...
Relative energy (cm <sup>-1</sup> )	0.0	6.1	519.3	...
MOPAC 6:				
Absolute energy (a.u.)	-47.040 630	-47.040 627	-47.038 839	-47.038 833
Relative energy (cm <sup>-1</sup> )	0.0	0.7	393.1	394.4
<i>Ab initio:</i>				
Internal angles (degrees)				
$\alpha_{10-8-7-11}$	24.5	-24.7	25.7	...
$\alpha_{9-8-7-5}$	26.7	-26.4	25.5	...

<sup>a</sup>6-31G\* basis set.<sup>b</sup>See Fig. 11.

and  $B$  is the rotational constant, methyl deuteration reduces  $B$  by a factor of two.) The spectra can be fit to the rotor Hamiltonian presented in Sec. III. The potential parameters are given in Table V and the potential and energy levels are plotted in Fig. 14. The results are best described [see Eq. (3)] by a potential with  $V_3=35$  cm<sup>-1</sup> and  $V_6=28$  cm<sup>-1</sup> using a rotational constant of  $B=5.2$  cm<sup>-1</sup> for the -CH<sub>3</sub> rotor and  $B=2.6$  cm<sup>-1</sup> for the -CD<sub>3</sub> rotor with the same  $V_3$  and  $V_6$ . The symmetry species of the levels using the  $G_6^2$  character table<sup>17</sup> are given in Table V. The doublet origin for the -CH<sub>3</sub> compound arises from an a-e energy difference of ca. 3.0 cm<sup>-1</sup> in the  $S_1$  state and nearly degenerate a-e (bound) rotor states in  $S_0$ . The  $V_3$  potential constant in the ground state is not known but is expected to be roughly 100 cm<sup>-1</sup>. The  $S_1$  zero point energy for the -CH<sub>3</sub> rotor is 27 cm<sup>-1</sup>.  $G_6^2$  selection rules give  $a_1 \rightarrow a_1$ ,  $a_2 \rightarrow a_2$ , and  $e \rightarrow e$  dipole allowed transitions.

The  $G_6^2$  group is chosen to be appropriate for the excited state based on the assumptions that the NH<sub>2</sub> group is freely rotating or inverting or that the NH<sub>2</sub> group is planar. Both of these assumptions are true for the  $S_1$  state of

aniline.<sup>19</sup> Since the  $a_1 \rightarrow a_2$  transition intensity is quite weak this appears to be a reasonable approximation. If the NH<sub>2</sub> group is not planar or freely inverting, the  $a_1 \rightarrow a_2$  transitions become allowed in the  $G_3^1$  group.

The intensities of the transitions are not fit in this work (the only way to get relative displacements between the methyl groups in  $S_1$  and  $S_0$ ), but one can judge from the large origin intensity and small intensity of features removed from the origin that the anticipated shift in position of the methyl groups in  $S_1$  and  $S_0$  is relatively small.

The spectra for 3-methylaniline are presented in Fig. 15. The methyl rotor features to the blue of the origin doublet are too weak to be assigned with confidence. Based solely on the appearance of an origin doublet, the ground state rotor may be bound and the excited state rotor relatively free, or the converse.

MOPAC calculations estimate a ground state methyl rotor barrier of 218 cm<sup>-1</sup> for 2-methylaniline and 8.4 cm<sup>-1</sup> for 3-methylaniline, indicating that the 3-methylaniline methyl rotor is bound in the excited state. Similar results

## 2-METHYLANILINES

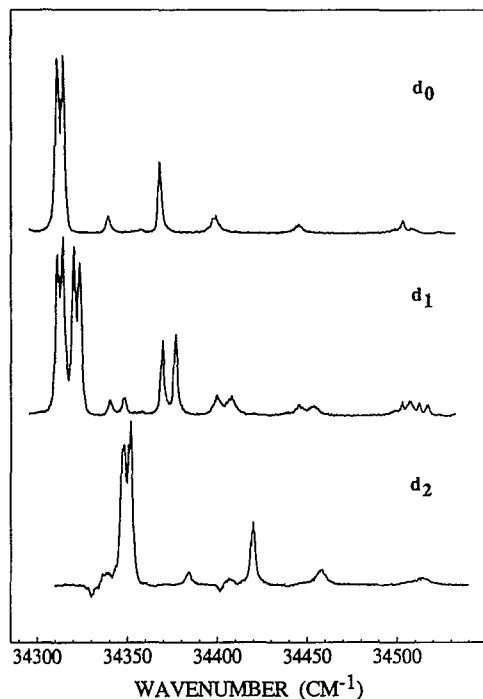


FIG. 12. MRES of the origin region of amino deuterated isotopomers of 2-methylaniline. The doublet origin arises from an *a-e* methyl rotor splitting in the excited state as suggested by the diverging progression to the blue of the origin.

## 2-METHYLANILINE

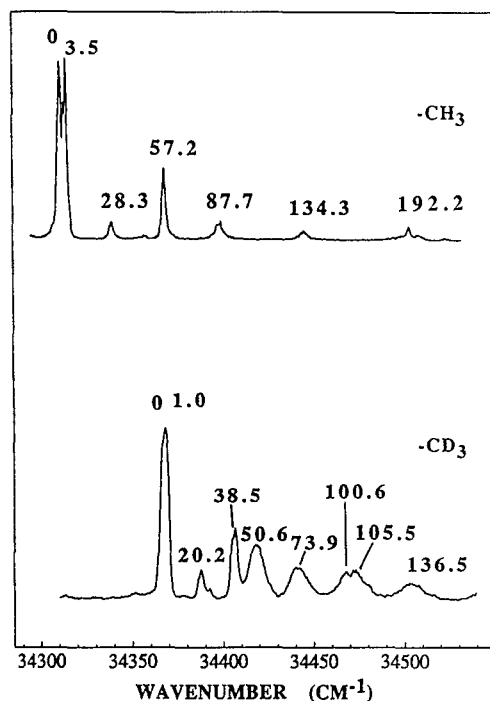


FIG. 13. The effect of methyl group deuteration is shown to decrease the rotor energy levels by roughly a factor of two.

TABLE V. 2-Methylaniline  $S_1$  rotor features.<sup>a</sup>

Transition <sup>b</sup>	CH <sub>3</sub> <sup>c</sup>		CD <sub>3</sub> <sup>d</sup>	
	Observed	Calculated	Observed	Calculated
0 <i>a</i> <sub>1</sub> →0 <i>a</i> <sub>1</sub>	0.0	0.0	0.0	0.0
0 <i>a</i> <sub>1</sub> →3 <i>a</i> <sub>2</sub>	(~45) <sup>e</sup>	47.3	...	31.1
0 <i>a</i> <sub>1</sub> →6 <i>a</i> <sub>1</sub>	192.2	192.1	105.5	103.0
1 <i>e</i> →1 <i>e</i>	3.5	3.14	1.5	0.56
1 <i>e</i> →2 <i>e</i>	28.3	28.5	20.2	23.8
1 <i>e</i> →4 <i>e</i>	87.7	88.5	50.6	51.4
1 <i>e</i> →5 <i>e</i>	134.3	134.9	73.9	74.6
1 <i>e</i> →7 <i>e</i>	...	259.4	136.5	136.3
1 <i>e</i> →8 <i>e</i>	...	337.3	181.4	175.2
0 <i>a</i> <sub>1</sub> →3 <i>a</i> <sub>1</sub>	57.2	57.4	38.5	37.2
0 <i>a</i> <sub>1</sub> →6 <i>a</i> <sub>2</sub>	(~195) <sup>e</sup>	191.7	100.6	102.4

<sup>a</sup> $V = (V_3/2)(1 - \cos 3\phi) + (V_6/2)(1 - \cos 6\phi)$  for which  $V_3 = 35.0 \text{ cm}^{-1}$ ,  $V_6 = 28.0 \text{ cm}^{-1}$ .

<sup>b</sup>The group for this level classification scheme is assumed to be  $G_6^2$  for the excited state. The NH<sub>2</sub> thus is assumed to be planar and/or to undergo torsional tunneling and inversion.

<sup>c</sup> $B = 5.2 \text{ cm}^{-1}$ .

<sup>d</sup> $B = 2.6 \text{ cm}^{-1}$ .

<sup>e</sup>Very weak features.

have been obtained for *meta*-xylene<sup>12</sup> and *meta*-fluorotoluene.<sup>15</sup>

The effect of the  $\text{-NHD/-NDH}$  bond inequivalence can still be observed for the 3-methylaniline- $d_1$  spectrum. Note that for the  $d_0$  and  $d_2$  spectra, the rotor *a-e* splitting of the  $0_0^0$  transition is resolved nearly to the base line while for the  $d_1$  species this splitting is barely resolved to the half intensity point. Even for methyl substitution in the meta position, the  $\text{-NHD/-NDH}$  inequivalence is observable.

Calculations for 2- and 3-methylaniline are presented in Table VI. In absolute energy 3-methylaniline is more

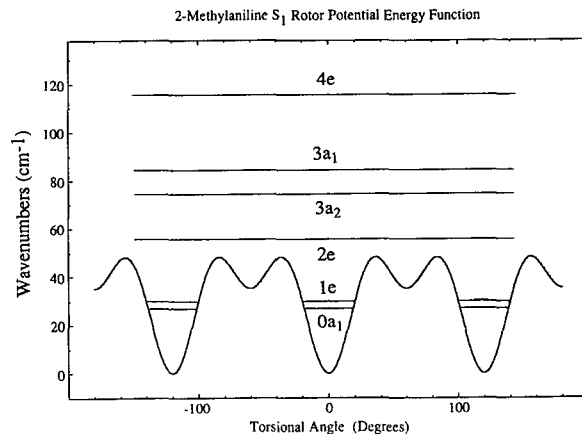
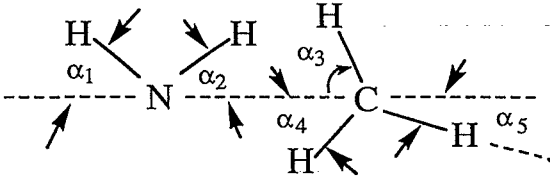


FIG. 14. Excited state methyl rotor potential energy function for 2-methylaniline as derived from a fit to rotor transitions. Potential constants used are  $V_3 = 35 \text{ cm}^{-1}$  and  $V_6 = 28 \text{ cm}^{-1}$ . A zero point energy of  $27 \text{ cm}^{-1}$  was calculated.

TABLE VI. Minimum energy geometry and structure of 2- and 3-methylaniline (energy in  $\text{cm}^{-1}$  and angles in degrees).


Molecular property	2-methylaniline		3-methylaniline	
	<i>Ab initio</i> <sup>a</sup>	MOPAC 6	<i>Ab initio</i> <sup>a</sup>	MOPAC 6
Absolute energy (a.u.)	-324.767 099	-41.544 23	-324.768 251	-41.546 09
Relative energy ( $\text{cm}^{-1}$ )	252.9	408.3	0.0	0.0
2- vs 3-methylaniline				
Internal angles (degrees)				
$\alpha_1$	18.0	27.2	27.0	30.0
$\alpha_2$	34.3	28.2	24.1	25.1
$\alpha_3$	65.7	61.2	75.8	72.5
$\alpha_4$	54.5	59.1	43.8	46.8
$\alpha_5$	5.3	1.0	15.7	12.6

<sup>a</sup>6-31G\* basis set.

stable than 2-methylaniline suggesting again a repulsive (steric) interaction between the two groups attached to the aromatic ring. The calculated energy minimum for both molecules has a methyl hydrogen atom away from the

amino group nearly in the plane of the ring in the  $S_0$  electronic state.

## V. CONCLUSIONS

Experimental and theoretical studies of substituted anilines with various side chain substituents have been reported. The major conclusions drawn from these studies are the following: (1) The two amino hydrogens are physically distinct in all compounds studied. (2) Substituent group torsional motion in  $S_1$  has been identified for all molecules except the 2-,3-methylanilines. (3) 2-methylaniline is shown to have a low barrier (ca.  $50 \text{ cm}^{-1}$ ) to methyl internal rotation in  $S_1$  and a high barrier in  $S_0$  ( $> 100 \text{ cm}^{-1}$ ). (4) The semiempirical and *ab initio* calculations presented here, for the most part, agree with experimental data and can be used to assign conformational structure and obvious low frequency modes. (5) Two conformers of 2-aminobenzyl alcohol are believed to exist in the supersonic expansion consistent with semiempirical calculational results. (6) Aromatic ring side-chain substituents with two heavy atoms undergo displacement in equilibrium torsional position upon  $S_1 \leftarrow S_0$  excitation, while methyl groups apparently do not, based on vibronic intensities.

## ACKNOWLEDGMENTS

The authors wish to thank Dr. Jeffrey I. Seeman and Dr. Henry V. Secor for helpful discussions of this work and synthetic efforts on the methyl deuterated compounds.

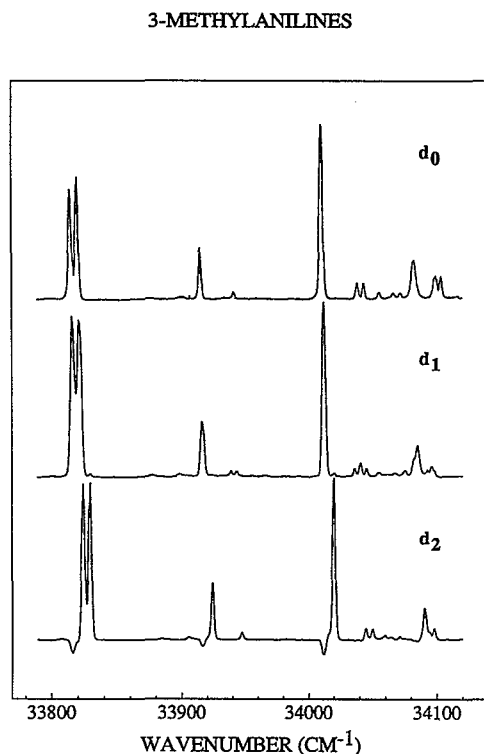


FIG. 15. MRES of amino deuterated isotopomers of 3-methylaniline. An apparent lack of rotor features to the right of the doublet origin suggests that the methyl rotor is either bound in  $S_0$  and relatively free in  $S_1$ , or the converse. The origin splitting does require that the two states have different potential barriers.

<sup>1</sup>H.-S. Im, E. R. Bernstein, J. I. Seeman, and H. V. Secor, *J. Am. Chem. Soc.* **113**, 4422 (1991); **112**, 7073 (1990).

<sup>2</sup>E. R. Bernstein, K. Law, and M. Schauer, *J. Chem. Phys.* **80**, 207 (1984).

- <sup>3</sup>K. H. J. Ling and R. P. Hanzlik, *Biochem. Biog. Res. Comm.* **160**, 844 (1989); J. I. Seeman and H. V. Secor (unpublished results).
- <sup>4</sup>MOPAC 6, J. J. P. Stewart, (Frank J. Seiler Research Laboratory, USAF, Colorado Springs, Colorado, 1990).
- <sup>5</sup>GAUSSIAN 88, M. J. Frisch, M. Head-Gordon, H. B. Schlegel, K. Raghavachari, J. S. Binkley, C. Gonzalez, D. J. Dufrees, D. J. Fox, R. A. Whiteside, R. Seeger, C. F. Meluis, J. Baker, R. L. Martin, L. R. Kahn, J. J. P. Stewart, E. M. Fluder, S. Topiol, and J. A. Pople (Gaussian Inc., Pittsburgh, Pennsylvania, 1989), MOPAC 4, J. J. P. Stewart (Frank J. Seiler Research Laboratory, USAF, Colorado Springs, Colorado, 1990), (6th ed.).
- <sup>6</sup>A. K. Rappé, C. J. Casewitt, K. S. Colwell, W. A. Goddard III, and W. M. Skiff, "WERK (also referred to as UFF), A Rule-Based Full Periodic Table Force Field for Molecular Mechanics and Molecular Dynamics Simulations," *J. Am. Chem. Soc.* (in press).
- <sup>7</sup>F. Miller, *Molecular Spectroscopy*, edited by P. Hepple (Inst. of Petroleum Res., London, 1968), and references therein.
- <sup>8</sup>T. Oka, *Molecular Spectroscopy: Modern Research*, edited by K. N. Rao (Academic, New York, 1976), Vol. II, and references therein.
- <sup>9</sup>J. D. Lewis, T. B. Malloy, Jr., T. H. Chao, and J. Laane, *Mol. Spectrosc.* **12**, 427 (1972).
- <sup>10</sup>K. Okuyama, N. Mikami, and M. Ito, *J. Phys. Chem.* **89**, 5617 (1985).
- <sup>11</sup>J. Susskind, *J. Chem. Phys.* **53**, 2492 (1970).
- <sup>12</sup>P. J. Breen, J. A. Warren, E. R. Bernstein, and J. I. Seeman, *J. Chem. Phys.* **87**, 1917, 1927 (1987).
- <sup>13</sup>J. Murakami, M. Ito, and K. Kaya, *Chem. Phys. Lett.* **80**, 203 (1981).
- <sup>14</sup>A. Oikawa, H. Abe, N. Mikami, and M. Ito, *J. Phys. Chem.* **88**, 5180 (1984).
- <sup>15</sup>K. Okuyama, N. Mikami, and M. Ito, *J. Phys. Chem.* **89**, 5617 (1985).
- <sup>16</sup>H. C. Longuet-Higgins, *Mol. Phys.* **6**, 445 (1963).
- <sup>17</sup>P. R. Bunker, *Molecular Symmetry and Spectroscopy* (Academic, New York, 1979).
- <sup>18</sup>S. Li, E. R. Bernstein, and J. I. Seeman, *J. Phys. Chem.* (submitted).
- <sup>19</sup>D. A. Chernoff and S. A. Rice, *J. Chem. Phys.* **70**, 2511 (1979).